Multiplet and lifetime effects in the $4d$ photoelectron spectrum of Eu

Ch. Gerth, K. Godehusen, M. Richter,* and P. Zimmermann
Institut für Atomare und Analytische Physik, Technische Universität Berlin, Hardenbergstrasse 36, D-10623 Berlin, Germany

J. Schulz, Ph. Wernet, and B. Sonntag
II. Institut für Experimentalphysik, Universität Hamburg, Luruper Chaussee 149, D-22761 Hamburg, Germany

A. G. Kochur and I. D. Petrov
Rostov State University of Transport Communication, Narodnogo Opolcheniya 2, Rostov-na-Donu, 344038 Russia
(Received 5 August 1999; published 12 January 2000)

A high-resolution $4d$ photoelectron spectrum of Eu has been measured. The spectrum reveals a rich structure reflecting multiplet splitting due to $4d$-$4f$, $4f$-$4f$, and spin-orbit interaction. In order to interpret the complex $4d^{-1}$ multiplet structure, calculations in the intermediate coupling scheme were performed taking into account the term-dependent lifetime width of each $4d^{-1}$ multiplet state. The strong influence of both the $4d$-$4f$ exchange interaction and the term-dependent lifetime broadening on the shape of the $4d$ photoelectron spectrum is demonstrated. Due to the inner-shell character of the $4d$ and $4f$ orbitals, the spectrum of atomic Eu is similar to that of Eu and Gd solid samples having the same $4f^7$ occupancy.

PACS number(s): 32.80.Fb

I. INTRODUCTION

The rare-earth elements with their open $4f$ shell have attracted interest for many decades and much work has been devoted to the study of the $4d$ photoelectron spectra. The physical origin and the appropriate description of the $4d^{-1}$ multiplet structures in rare-earth elements have been the subject of a long-standing controversy. One of the reasons was that the $4d$ photoelectron spectra of lanthanides are spread over an energy range of more than 30 eV. The spectra can roughly be divided into a low ionization energy region and a high ionization energy region. The high ionization energy regions only comprise weak features that were often overlooked. Early experimental studies on rare-earth compounds [1] and metals [2] only dealt with the low ionization energy region of the $4d$ photoelectron spectra.

The spectra of the elements at the beginning and the end of the lanthanide series exhibit complex structures at low ionization energies. On the other hand, the low ionization energy parts in the spectra of the atoms at the center of the series—Eu and Gd—were found to have very simple doublet structures with splittings resembling the spin-orbit splitting of the $4d$ core hole. Hence, this splitting in $4d$ photoelectron spectra of atomic Eu [3] and solid EuO [1] was ascribed to spin-orbit interaction. Kowalczyk *et al.* [2] were able to partly resolve the fine structure in the spectrum of solid Eu and attributed the splitting to the $4d$-$4f$ electrostatic interaction: the two peaks were assigned to $4d^9 4f^7(^8S)^7D$ and ^9D multiplets.

Calculations performed by Demekhin *et al.* [4] for all rare-earth atoms and later by Pan *et al.* [5] for Eu revealed a large $4d^{-1}$ multiplet splitting of about 30 eV due to the strong $4d$-$4f$ electrostatic interaction, while the $4d^{-1}$ spin-orbit interaction only accounted for a fine-structure splitting of a few eV. Based on the calculations by Pan *et al.* [5], the entire low ionization energy region was assigned to ^9D states in the early photoelectron spectra of atomic Eu excited by synchrotron radiation [6]. The results of term-dependent calculations for the $4d$-$4f4f$ super-Coster-Kronig (SCK) decay rates of the $4d^{-1}$ multiplet states led Ogasawara *et al.* [7] to the same assignment. They found the natural widths to be very small in the low ionization energy region of the $4d^{-1}$ multiplet and ascribed the corresponding states to $4d^9 4f^7(^8S)\ ^9D$ states since the intense $4d$-$4f4f$ SCK decay, which leads to $4d^{10}4f^5(^6L)\epsilon\ell\ ^7L$ states, is forbidden for these ^9D high-spin states. This dependence of the decay process upon the total spin has been exploited in the studies of the low ionization energy region of the $4d^{-1}$ multiplet by means of photoelectron-ion coincidence spectroscopy ([8], and references therein). Only one peak of the doublet was found to comprise ^9D high-spin states, whereas the other peak mainly reflects $4d^9 4f^7(^6L)\ ^7D$ character.

In this paper we report on high-resolution $4d$ photoelectron spectra of atomic Eu. The vanishing total angular momentum in the ground state due to the half-filled $4f$ shell results in a simplification of the $4d^{-1}$ multiplet. Furthermore, the $4f^7\ ^8S_{7/2}$ ground state is so stable that it is conserved in Eu and Gd metal. We calculate the natural widths considering every possible Auger decay of each $4d^{-1}$ multiplet state. Radiative decay of the $4d^{-1}$ states can be neglected [9].

II. EXPERIMENT

A beam of free Eu atoms was produced using a resistively heated oven and ionized by linearly polarized undulator ra-

*Permanent address: PTB/BESSY, Albert-Einstein-Strasse 15, D-12485 Berlin, Germany.

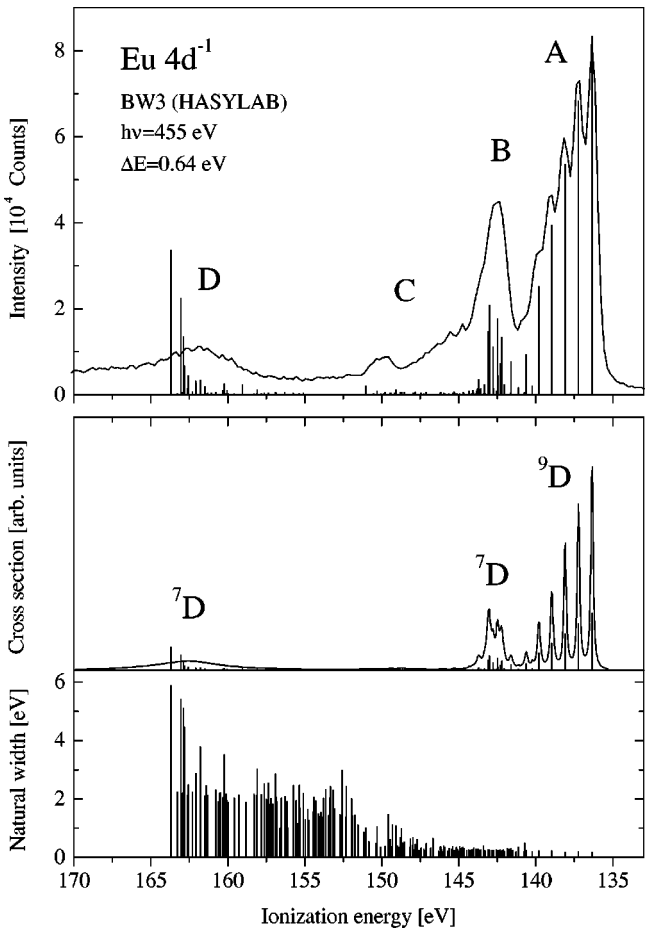

FIG. 1. Top: experimental $4d$ photoelectron spectrum of Eu recorded at a photon energy of 455 eV together with a calculated bar spectrum. Middle: calculated photoionization cross section for each multiplet state (bar spectrum); calculated spectrum taking into account the natural width. Bottom: calculated natural width of each multiplet state.

diation. The photoelectrons emerging from the interaction region were detected by a SCIENTA SES200 spherical electron analyzer. The analyzer only accepted electrons with an angle of emission close to the magic angle 54.7° relative to the polarization axis of the synchrotron radiation. The photoelectron spectra were recorded at a fixed photon energy $h\nu$, while scanning the accelerating (retarding) lens voltage of the analyzer.

The spectrum of Fig. 1 was measured at the SX-700 monochromator of the BW3 undulator station at HASYLAB in Hamburg. The spectrum was taken at a photon energy of 455 eV with a total instrumental bandwidth of 0.64 eV [full width at half maximum (FWHM)]. A total instrumental bandwidth of 0.42 eV (FWHM) was achieved in the case of the spectrum presented in Fig. 2, which was recorded at a photon energy of 165 eV at the undulator beamline TGM 5 at BESSY in Berlin. For the determination of the photon energy and the instrumental bandwidth and for the calibration of the ionization energy scale we used $3p$ photoelectron spectra of argon.

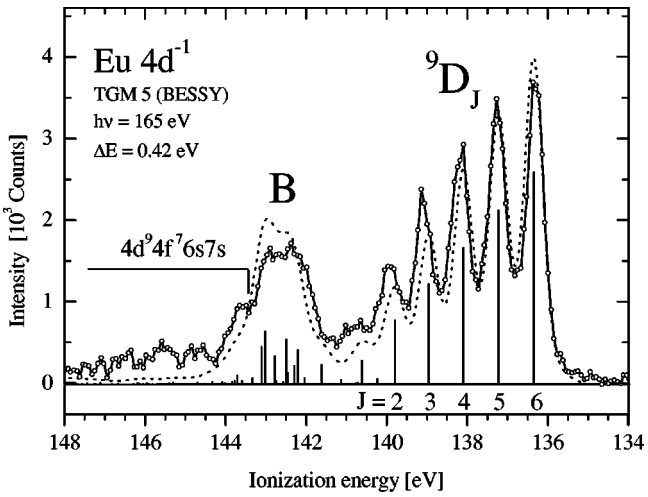

FIG. 2. High-resolution $4d$ photoelectron spectrum of atomic Eu. The spectrum shows the low ionization energy region. The dotted line was obtained by convoluting the calculated spectrum of Fig. 1 with a Gaussian of 0.42 eV (FWHM) corresponding to the total experimental bandwidth.

III. METHOD OF CALCULATION

The $4d$ photoionization cross sections were obtained using the $4d^9 4f^7(EJ)$ final states calculated in the intermediate coupling scheme as described in [10]. In order to account for many-electron correlations and to get the best agreement with the experiment, the Slater integrals of the $4f$-$4f$ and $4d$-$4f$ interactions were scaled with factors 0.8 and 0.7, respectively. The natural level widths of the final ionic states Eu II $4d^{-1}(EJ)$ were determined by calculating the partial widths for all possible nonradiative decays. The total width of each component is then given by the sum over all partial widths of the transitions $4d^{-1} \rightarrow n_1 l_1^{-1}, n_2 l_2^{-1} \varepsilon\ell$ that are energetically allowed:

$$\Gamma(4d^{-1}(EJ)) = \sum_{n_1 l_1, n_2 l_2, E'J', \ell} \Gamma(4d^{-1}(EJ) \rightarrow n_1 l_1^{-1} n_2 l_2^{-1}(E'J')\varepsilon\ell). \quad (1)$$

The Auger electron wave functions $\varepsilon\ell$ were calculated in the Hartree-Fock approximation. For the Auger electron energies the calculated differences of mean Hartree-Fock-Pauli energies of initial- and final-state configurations of the core were taken.

IV. RESULTS AND DISCUSSION

The upper part of Fig. 1 shows the $4d$ photoelectron spectrum of Eu recorded at a photon energy of 455 eV. The bar spectrum in the middle part of the figure represents the calculated photoionization cross section for each component of the $4d^{-1}$ multiplet. In the lower panel the corresponding linewidth, determined from the Auger decay rate for each $4d^{-1}$ state, is shown. The solid line in the middle panel represents a calculated $4d$ photoelectron spectrum. It was obtained by replacing each bar by a Lorentzian profile with

TABLE I. Characteristics of the 20 most intense lines of the calculated Eu 4*d* photoelectron spectrum (total number of components is 238). The spectrum was calculated with Slater integrals scaled by 0.7 and 0.8 for the 4*d*-4*f* and 4*f*-4*f* interaction, respectively. The accuracy of the experimental ionization energies amounts to ±0.2 eV.

Region	Calculated energies (eV)	Dominant contribution [a] (*LSJ*)	Relative intensity (arb. units)	Natural width (eV)	Experimental energies (eV)
A	136.32 [b]	0.985 $^9D_6$	1.000	0.17	136.32
	137.20	0.935 $^9D_5$	0.820	0.18	137.26
	138.07	0.878 $^9D_4$	0.642	0.17	138.19
	138.93	0.810 $^9D_3$	0.472	0.21	139.08
	139.77	0.696 $^9D_2$	0.296	0.23	139.89
B	140.59	0.685 $^7D_1$	0.112	0.24	142.6[c]
	141.58	0.577 $^7P_2$	0.091	0.29	
	142.18	−0.550 $^7D_2$	0.160	0.22	
	142.27	0.568 $^7P_4$	0.086	0.25	
	142.42	−0.425 $^7D_3$	0.053	0.02	142.6 [c]
	142.46	−0.490 $^7D_3$	0.211	0.21	
	142.75	−0.469 $^7D_5$	0.133	0.23	
	142.99	0.491 $^7D_4$	0.249	0.25	
	143.08	0.401 $^7D_5$	0.176	0.25	
	143.68	−0.393 $^7F_5$	0.042	0.23	
D	162.54	0.679 $^5G_4$	0.053	2.48	162.0[c]
	162.79	0.447 $^7D_2$	0.079	4.45	
	162.80	−0.553 $^5P_1$	0.034	4.04	
	162.84	0.536 $^7D_3$	0.161	5.08	
	163.02	0.611 $^7D_4$	0.269	5.40	
	163.65	0.677 $^7D_5$	0.402	5.88	

[a] *LSJ* terms of configuration $4d^9 4f^7$ giving the largest contributions to the final-state vector.
[b] Ionization energy of this line was matched to the experimental value.
[c] For peaks *B* and *D*, only the energies of the center are given.

an area equal to the photoionization cross section and a width equal to the calculated linewidth.

The spectrum exhibits a large multiplet splitting of about 30 eV and can roughly be divided into four groups of lines (*A*–*D*). The linewidths differ by more than one order of magnitude and increase with increasing ionization energies. The spectrum nicely demonstrates the influence of the term-dependent decay width on the shape of the 4*d* photoelectron spectrum: The intensity of the peak *D* at high ionization energies is considerably smeared out. This strong broadening is mainly caused by intense 4*d*-4*f*4*f* SCK transitions. In contrast, the fine-structure components of peak *A* are resolved documenting their much smaller linewidth.

The calculated photoionization cross section and natural width of the 20 strongest lines are summarized in Table I. For each line, the leading contribution of the *LSJ* terms of the configuration Eu II $4d^9 4f^7$ to the final-state vector is given. The ionization energy scale of the calculated spectrum has been matched to that of the measured spectrum at the energy of the $^9D_6$ state.

According to our calculations, the splitting of the $4d^{-1}$ multiplet is dominated by the 4*d*-4*f* electrostatic interaction. For the groups *A* and *D*, the spin of the $4d^{-1}$ core hole couples parallel and antiparallel to the large total spin of the $4f^7$ $^8S_{7/2}$ state. The lines of group *B* mainly consist of low-spin ^7D states, given by parallel coupling of the core-hole spin to the angular momenta of $4f^7$ ^6L states. Here, a recoupling of the 4*f* shell occurs in the photoionization process. In the region *D*, not only $(^8S)^7D$ states but also weak ^5L states with the core-hole spin coupled antiparallel to the recoupled 4*f* shell contribute to the spectrum.

An additional feature that is missing in the calculated spectrum is apparent in the experimental spectrum in region *C* at ionization energies between 144 eV and 151 eV. The structure of this region strikingly resembles the groups *A* and *B* and can therefore be ascribed to the corresponding $4d^9 4f^7 6s7s$ satellite lines. Here, a 6*s* electron is exited into the 7*s* shell. The shift of 7.3 eV to higher ionization energies is in accordance with the shift of the corresponding $4f^6 6s7s(^7F)$ satellite line in the 4*f* photoelectron spectrum [6].

In order to study the fine-structure splitting of the ^9D high-spin states, the low ionization energy region of the 4*d* photoelectron spectrum was measured with enhanced resolution. The spectrum was recorded at a photon energy of 165 eV and is depicted in Fig. 2. The experimental spectrum is shown together with the bar spectrum and the calculated

spectrum (dotted line), for which the instrumental bandwidth was taken into account. The fine structure of peak *A* was resolved experimentally, since the natural width of the ^9D multiplet states is small compared to their spacing. This is well reproduced in the calculated spectrum. The fine-structure components localized within peak *B* are strongly mixed due to the $4f$-$4f$ electrostatic and the spin-orbit interaction. Small deviations between the calculated and the measured spectrum may result from configuration interaction, which was neglected in the calculation. The prominent shoulder at the high ionization energy side of peak *B* belongs to group *C* in Fig. 1 and originates from the $4d^9 4f^7 6s7s^9D_6$ satellite emission. The ionization energies determined from the experimental spectra are included in Table I and are in reasonable agreement with the calculated values; for peaks *B* and *D* only the energies of the center are given.

Due to the fact that the $4d$ and $4f$ electrons are localized in the atomic core and the $4d^{-1}$ multiplet splitting is dominated by the $4d$-$4f$ electrostatic interaction, the $4d$ photoionization of rare-earth metals and compounds is strongly influenced by atomic effects. Atomic Eu is a key element for the comparison with its solid-state $4f^7$ counterparts Eu and Gd, because of its well-separated $^8S_{7/2}$ ground state that is preserved in the metal. Furthermore, thermal population of initial states can be neglected at evaporation temperatures necessary for the production of an atomic beam.

Figure 3 depicts our $4d$ photoelectron spectrum of atomic Eu together with the $4d$ photoelectron spectrum of trivalent Gd(0001) from Ref. [11], which was measured with linearly polarized synchrotron radiation at a photon energy of 400 eV at room temperature. Both spectra are shown for an energy region of 46 eV; the atomic Eu spectrum was shifted by 4.4 eV to give the best overlap with the solid Gd spectrum in the rising slope of peak *A*. The energy scale of the top axis corresponds to the Gd spectrum while the energy scale of the bottom axis belongs to Eu.

The Gd spectrum closely resembles that of Eu and displays the same principal features *A*, *B*, and *D*. The most striking difference between both spectra is the background of secondary electrons in the Gd spectrum that increases smoothly above the lowest $4d^{-1}$ threshold. Another notable difference between the Eu and Gd spectra is the greater $A-D$ splitting of the latter, originating from the larger values of the $4d$-$4f$ exchange interaction integrals in Gd.

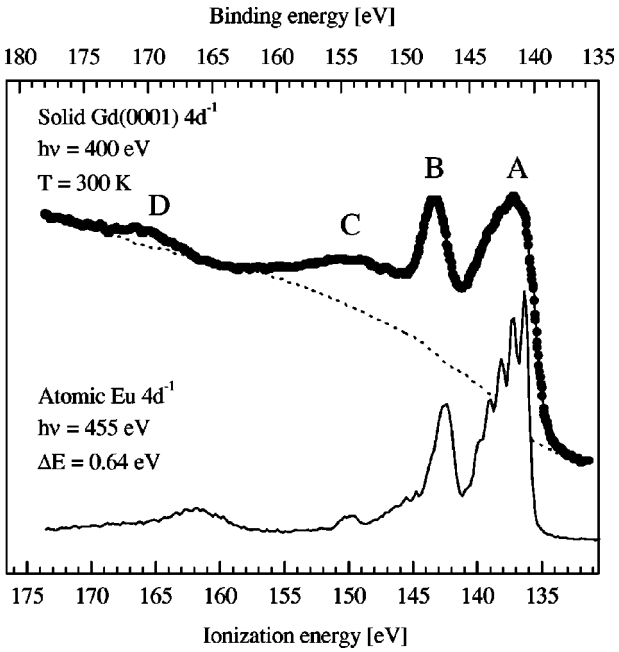

FIG. 3. Comparison between the $4d$ photoelectron spectra of atomic Eu and metal Gd; the Gd spectrum was taken from van der Laan *et al.* [11].

As can be seen from Fig. 3, the broad structure *C* in the Gd spectrum differs considerably from that in the Eu spectrum. The binding in Gd metal is mainly caused by the $6s$ and $5d$ electrons leading to a delocalization of the $6s$ electrons accompanied with the formation of the conduction band. Therefore, the simultaneous excitation of the outer electrons in Gd metal is not expected to lead to a sharp satellite structure as observed in the spectrum of atomic Eu. Our findings corroborate the atomic interpretation of the $4d$ photoelectron spectrum of Gd metal proposed by Lademann *et al.* [12]. These authors ascribed the peak *C* to an extrinsic energy loss.

ACKNOWLEDGMENTS

One of the authors (A.G.K.) would like to thank TU Berlin for hospitality during his stay in Berlin. The authors are thankful to the staff at BESSY and HASYLAB for their assistance. The financial support of the DFG is gratefully acknowledged.

[1] A. J. Signorelli and R. G. Hayes, Phys. Rev. B **8**, 81 (1973).
[2] S. P. Kowalczyk, N. Edelstein, F. R. McFeely, L. Ley, and D. A. Shirley, Chem. Phys. Lett. **29**, 491 (1974).
[3] C. S. Fadley and D. A. Shirley, Phys. Rev. A **2**, 1109 (1970).
[4] V. F. Demekhin, S. A. Yavna, Yu. I. Bairachnyi, and V. L. Sukhorukov, J. Struct. Chem. **18**, 513 (1977) [translated from Zh. Struk. Khim. **18**, 644 (1977)].
[5] C. Pan, S. L. Carter, and H. Kelly, J. Phys. B **20**, L335 (1987).
[6] M. Richter, M. Meyer, M. Pahler, T. Prescher, E. von Raven, B. Sonntag, and H.-E. Wetzel, Phys. Rev. A **40**, 7007 (1989).
[7] H. Ogasawara, A. Kotani, and B. T. Thole, Phys. Rev. B **50**, 12 332 (1994).
[8] Ch. Gerth, A.G. Kochur, M. Groen, T. Luhmann, M. Richter, and P. Zimmermann, Phys. Rev. A **57**, 3523 (1998).
[9] T. Luhmann, Ch. Gerth, M. Martins, M. Richter, and P. Zimmermann, Phys. Rev. Lett. **76**, 4320 (1996).
[10] A. G. Kochur, V. L. Sukhorukov, and I. D. Petrov, J. Phys. B **29**, 4565 (1996).
[11] G. van der Laan, E. Arenholz, E. Navas, A. Bauer, and G. Kaindl, Phys. Rev. B **53**, R5998 (1996).
[12] W. J. Lademan, A. K. See, L. E. Klebanoff, and G. van der Laan, Phys. Rev. B **54**, 17 191 (1996).